Engineering Analysis with Boundary Elements 16 (1995) 333–340

0955-7997/95/$09.50

ELSEVIER

0955-7997(95)00078-X

Dual boundary integral equations for exterior problems

J. T. Chen, M. T. Liang & S. S. Yang

Department of Harbor and River Engineering, Taiwan Ocean University, Keelung, Taiwan

(Received 28 July 1995; revised version received 3 November; accepted 8 November 1995)

A dual integral formulation for the interior problem of the Laplace equation with a smooth boundary is extended to the exterior problem. Two regularized versions are proposed and compared with the interior problem. It is found that an additional free term is present in the second regularized version of the exterior problem. An analytical solution for a benchmark example in ISBE is derived by two methods, conformal mapping and the Poisson integral formula using symbolic software. The potential gradient on the boundary is calculated by using the hypersingular integral equation except on the two singular points where the potential is discontinuous instead of failure in ISBE benchmarks. Based on the matrix relations between the interior and exterior problems, the BEPO2D program for the interior problem can be easily reintegrated. This benchmark example was used to check the validity of the dual integral formulation, and the numerical results match the exact solution well.

Key words: Dual boundary integral equations, dual boundary element method, regularized method, exterior problem.

INTRODUCTION

A dual integral formulation for crack problems was developed in 1986[1] and published in 1988;[2] furthermore, it was extended to the Laplace equation with a degenerate boundary.[3,4] This numerical implementation was termed the dual boundary element method (DBEM) by Portela *et al.*,[5] and a large number of DBEM papers were published in this decade, e.g. Refs 4, 6–9. Three versions of dual boundary integral equations were suggested in Ref. 10. These formulations had been mainly applied to interior problems.[1–5,10,11] However, an exterior problem frequently occurs in the descriptions of many engineering problems, so the ability to handle this situation is not trivial. The exterior problem introduces an infinite boundary, and whether the integral along this infinite boundary vanishes or not in the third version of dual boundary integral equations will be investigated.

In this paper, the three versions of dual boundary integral equations for the interior problem in Ref. 10 are extended to the exterior problem, and the difference between the interior and exterior problems on the influence matrix will be discussed. An example with series-form and closed-form solutions is shown to check the validity of the present DBEM formulation, and the results of the DBEM solution are achieved by modifying the program, BEPO2D, for the interior problem from the original interior to the exterior problem since the relations between the influence matrix of the interior problem and that of the exterior problem can be found. Also, the potential gradient on the boundary point is determined by the second equation of dual integral equations instead of failure in ISBE benchmarks.[12]

REVIEW OF DUAL BOUNDARY INTEGRAL EQUATIONS FOR INTERIOR PROBLEMS

Chen and Hong[10] derived three versions of the dual boundary integral equations for interior problems as follows:

Version I (unregularized form):

$$\pi u(x) = \mathrm{CPV}\int_B T^{\mathrm{i}}(s,x)u(s)\,\mathrm{d}B(s) - \mathrm{RPV}\int_B U^{\mathrm{i}}(s,x)t(s)\,\mathrm{d}B(s) \qquad (1)$$

$$\pi t(x) = \mathrm{HPV}\int_B M^{\mathrm{i}}(s,x)u(s)\,\mathrm{d}B(s) - \mathrm{CPV}\int_B L^{\mathrm{i}}(s,x)t(s)\,\mathrm{d}B(s) \qquad (2)$$

where x is on the boundary B, u and t are the potential and flux, U^i, T^i, L^i and M^i are the four kernels in the dual integral equations for the interior problems, and RPV, CPV and HPV denote the Riemann principal value, Cauchy principal value and Hadamard principal value, respectively.

Version II (regularized form with respect to u):

$$0 = \text{RPV}\int_B T^{\text{i}}(s,x)[u(s)-u(x)]\,\mathrm{d}B(s) - \text{RPV}\int_B U^{\text{i}}(s,x)t(s)\,\mathrm{d}B(s) \quad (3)$$

$$\pi t(x) = \text{CPV}\int_B M^{\text{i}}(s,x)[u(s)-u(x)]\,\mathrm{d}B(s) - \text{CPV}\int_B L^{\text{i}}(s,x)t(s)\,\mathrm{d}B(s) \quad (4)$$

Version III (regularized form with respect to t):

$$0 = \text{RPV}\int_B T^{\text{i}}(s,x)[u(s)-u(x) - u'(x)r_i\bar{s}_i - t(x)r_i\bar{n}_i]\,\mathrm{d}B(s) - \text{RPV}\int_B U^{\text{i}}(s,x)[t(s)-u'(x)n_i\bar{s}_i - t(x)n_i\bar{n}_i]\,\mathrm{d}B(s) \quad (5)$$

$$0 = \text{RPV}\int_B M^{\text{i}}(s,x)[u(s)-u(x) - u'(x)r_i\bar{s}_i - t(x)r_i\bar{n}_i]\,\mathrm{d}B(s) - \text{RPV}\int_B L^{\text{i}}(s,x)[t(s)-u'(x)n_i\bar{s}_i - t(x)n_i\bar{n}_i]\,\mathrm{d}B(s) \quad (6)$$

where $r_i = s_i - x_i$, u' denotes the tangent derivative of u along boundary B, n_i and $\bar{n}_i$ are the ith components of the outnormal vector on s and on x, and $\bar{s}_i$ is the ith component of the tangent vector on x. It must be noted that the free terms of the third version at the left hand side of the equalities in eqns (5) and (6) vanish. However, this is not the case as is easily seen in the exterior problem which will be elaborated on later.

DUAL BOUNDARY INTEGRAL EQUATIONS FOR EXTERIOR PROBLEMS

Extending eqns (1)–(6) of the interior problem to the exterior problem by considering the regularity condition at infinity for the integral on the infinite boundary B_∞,[13] we have:

Version I (unregularized form):

$$\pi u(x) = \text{CPV}\int_B T^{\text{e}}(s,x)u(s)\,\mathrm{d}B(s) - \text{RPV}\int_B U^{\text{e}}(s,x)t(s)\,\mathrm{d}B(s) \quad (7)$$

$$\pi t(x) = \text{HPV}\int_B M^{\text{e}}(s,x)u(s)\,\mathrm{d}B(s) - \text{CPV}\int_B L^{\text{e}}(s,x)t(s)\,\mathrm{d}B(s) \quad (8)$$

where the superscript 'e' denotes the exterior problem.

Version II (regularized form with respect to u):

$$0 = \text{RPV}\int_B T^{\text{e}}(s,x)[u(s)-u(x)]\,\mathrm{d}B(s) - \text{RPV}\int_B U^{\text{e}}(s,x)t(s)\,\mathrm{d}B(s) \quad (9)$$

$$\pi t(x) = \text{CPV}\int_B M^{\text{e}}(s,x)[u(s)-u(x)]\,\mathrm{d}B(s) - \text{CPV}\int_B L^{\text{e}}(s,x)t(s)\,\mathrm{d}B(s) \quad (10)$$

Version III (regularized form with respect to t):

$$2\pi u(x) = \text{RPV}\int_B T^{\text{e}}(s,x)[u(s)-u(x) - u'(x)r_i\bar{s}_i - t(x)r_i\bar{n}_i]\,\mathrm{d}B(s) - \text{RPV}\int_B U^{\text{e}}(s,x)[t(s)-u'(x)n_i\bar{s}_i - t(x)n_i\bar{n}_i]\,\mathrm{d}B(s) \quad (11)$$

$$2\pi t(x) = \text{RPV}\int_B M^{\text{e}}(s,x)[u(s)-u(x) - u'(x)r_i\bar{s}_i - t(x)r_i\bar{n}_i]\,\mathrm{d}B(s) - \text{RPV}\int_B L^{\text{e}}(s,x)[t(s)-u'(x)n_i\bar{s}_i - t(x)n_i\bar{n}_i]\,\mathrm{d}B(s) \quad (12)$$

Comparing eqns (1)–(6) with eqns (7)–(12), it is found that the free terms are different for version III between the interior (eqns (5) and (6)) and exterior problems (eqns (11) and (12)) although they are the same for the other two versions.

Proof of eqn (11):

Setting a reference solution as

$$u_{\text{r}}(\bar{x}) = u(x) + r_i u_{,i}(x) \quad (13)$$

where $r_i = \bar{x}_i - x_i$, we have

$$\nabla_{\bar{x}}^2 u_r(\bar{x}) = 0 \quad (14)$$

Also, $u(\bar{x})$ satisfies the Laplace equation, i.e.

$$\nabla_{\bar{x}}^2 u(\bar{x}) = 0 \quad (15)$$

Subtracting eqn (14) from eqn (15), the function $u(\bar{x}) - u_r(\bar{x})$ also satisfies the Laplace equation as follows:

$$\nabla_{\bar{x}}^2 (u(\bar{x}) - u_{\text{r}}(\bar{x})) = 0 \quad (16)$$

Based on the theory of dual integral equations for an exterior problem, we have

$$2\pi[u(\bar{x}) - u_r(\bar{x})] = \int_{B+B_\infty} T(s,\bar{x})[u(s) - u_r(s)]\,dB(s) - \int_{B+B_\infty} U(s,\bar{x})[t(s) - t_r(s)]\,dB(s) \tag{17}$$

Let $\bar{x}$ approaches x, eqn (17) reduces to

$$2\pi[u(x) - u_r(x)] = \int_{B+B_\infty} T(s,x)[u(s) - u_r(s)]\,dB(s) - \int_{B+B_\infty} U(s,x)[t(s) - t_r(s)]\,dB(s) \tag{18}$$

Since $u(\bar{x})$ is equal to $u_r(\bar{x})$ as x approaches $\bar{x}$ in eqn (13), we have

$$0 = \int_{B+B_\infty} T^e(s,x)[u(s) - u_r(s)]\,dB(s) - \int_{B+B_\infty} U^e(s,x)[t(s) - t_r(s)]\,dB(s) \tag{19}$$

It should be noted that integrations $\int_{B+B_\infty} T^e(s,x) \times [u(s) - u_r(s)]\,dB(s)$ and $\int_{B+B_\infty} U^e(s,x)[t(s) - t_r(s)]\,dB(s)$ do not vanish although $u(s)$ approaches $u_r(s)$ and $t(s)$ approaches $t_r(s)$ since the kernels $T^e(s,x)$ and $U^e(s,x)$ are both singular. For the exterior problem, the domain D is enclosed by the boundaries B and B_∞. Considering the contribution of integration over B_∞, we have

$$\begin{aligned}
&\int_{B_\infty} T^e(s,x)[u(s) - u_r(s)]\,dB(s) - \int_{B_\infty} U^e(s,x)[t(s) - t_r(s)]\,dB(s) \\
&= -\int_{B_\infty} [T^e(s,x)u_r(s) - U^e(s,x)t_r(s)]\,dB(s) \\
&= -\int_D \{[U^e_{,i}(s,x)u_r(s)]_{,i} - [U^e(s,x)u_{r,i}(s)]_{,i}\}\,dD(s) \\
&= -\int_D U^e_{,ii}u_r(s)\,dD(s) \\
&= -\int_D 2\pi\delta(x-s)u_r(s)\,dD(s) \\
&= -2\pi u_r(x) = -2\pi u(x)
\end{aligned} \tag{20}$$

Equation (11) is therefore proved. By taking the derivative with respect to eqn (11), we have eqn (12).

RELATIONS OF THE INTERIOR AND EXTERIOR PROBLEM

The linear algebraic equations for an interior problem discretized from the dual boundary integral equations can be written as

$$[T^i_{pq}]\{u_q\} = [U^i_{pq}]\{t_q\} \tag{21}$$

$$[M^i_{pq}]\{u_q\} = [L^i_{pq}]\{t_q\} \tag{22}$$

where $\{u_q\}$ and $\{t_q\}$ are the boundary potential and flux, and the subscripts p and q correspond to the labels of the collocation element and integration element, respectively.

For the exterior problem, we have

$$[T^e_{pq}]\{u_q\} = [U^e_{pq}]\{t_q\} \tag{23}$$

$$[M^e_{pq}]\{u_q\} = [L^e_{pq}]\{t_q\} \tag{24}$$

The influence coefficients of the four square matrices $[U]$, $[T]$, $[L]$ and $[M]$ can be represented as

$$U_{pq} = \mathrm{RPV}\int_{B_q} U(s_q,x_p)\,dB(s_q) \tag{25}$$

$$T_{pq} = \bar{T}_{pq} - 2\pi\delta_{pq} = -\pi\delta_{pq} + \mathrm{CPV}\int_{B_q} T(s_q,x_p)\,dB(s_q) \tag{26}$$

$$L_{pq} = \bar{L}_{pq} + 2\pi\delta_{pq} = \pi\delta_{pq} + \mathrm{CPV}\int_{B_q} L(s_q,x_p)\,dB(s_q) \tag{27}$$

$$M_{pq} = \mathrm{HPV}\int_{B_q} M(s_q,x_p)\,dB(s_q) \tag{28}$$

where B_q denotes the qth element and $\delta_{pq} = 1$ if $p = q$, otherwise it is zero; T_{pq} and $\bar{T}_{pq}$ differ by a jump term $-2\pi\delta_{pq}$ while L_{pq} and $\bar{L}_{pq}$ differ by a jump term $2\pi\delta_{pq}$. The explicit form will be derived in the following section. According to the dependence of the outnormal vectors in these four kernel functions for the interior

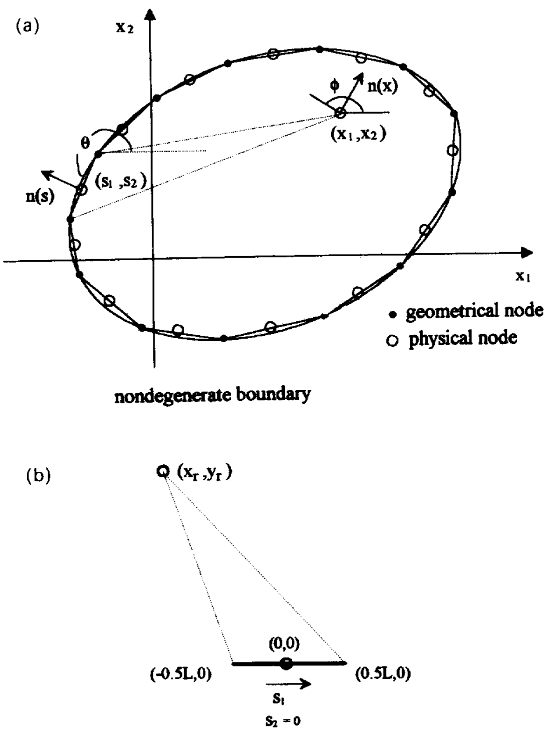

Fig. 1. (a) Boundary element discretization. (b) Coordinate transformation.

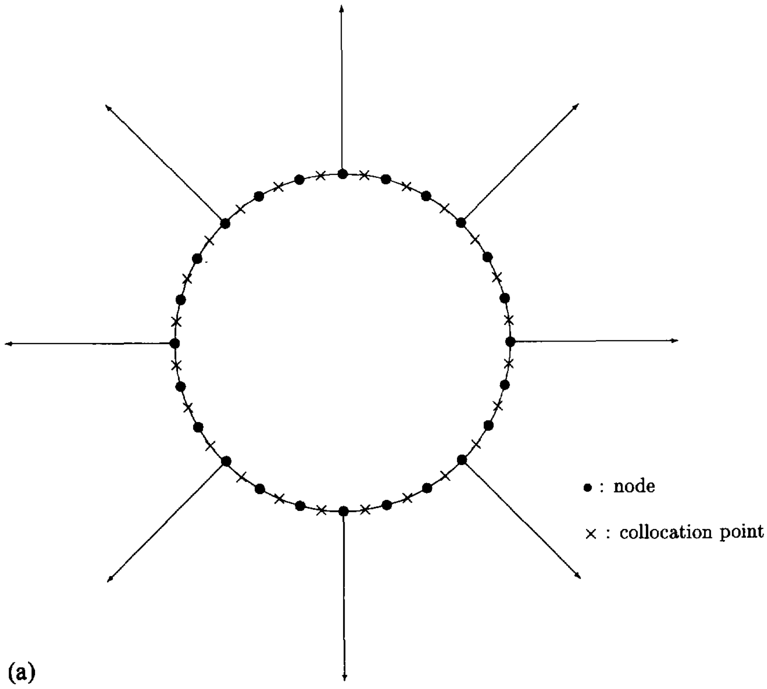

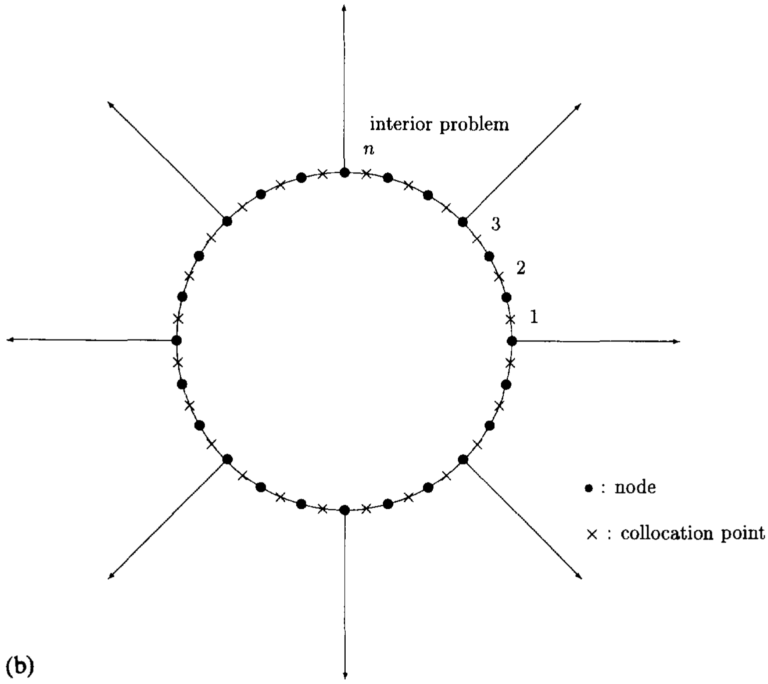

Fig. 2. (a) Boundary element mesh along the circular boundary. (b) Boundary element connectivity for the interior problem. (c) Boundary element connectivity for the exterior problem.

and exterior problems, their relationships can be easily found:

$$U^{i}_{pq} = U^{e}_{pq} \tag{29}$$

$$M^{i}_{pq} = M^{e}_{pq} \tag{30}$$

$$T^{i}_{pq} = \begin{cases} -T^{e}_{pq}, & \text{if } p \neq q \\ T^{e}_{pq}, & \text{if } p = q \end{cases} \tag{31}$$

$$L^{i}_{pq} = \begin{cases} -L^{e}_{pq}, & \text{if } p \neq q \\ L^{e}_{pq}, & \text{if } p = q \end{cases} \tag{32}$$

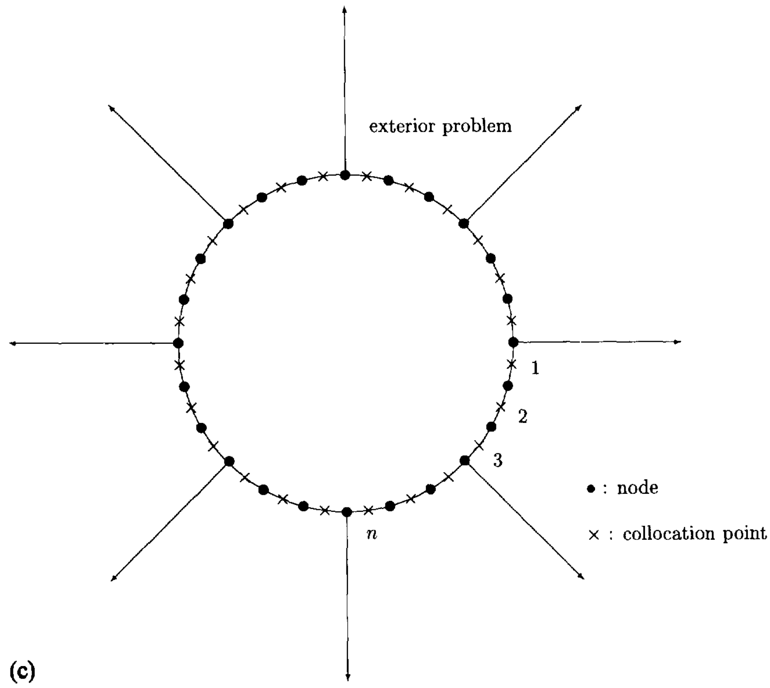

Fig. 2. *contd.*

CALCULATION OF POTENTIAL GRADIENT ON THE BOUNDARY POINT

Before solving for the potential on the interior point, the potential gradient on the interior point, and the potential gradient on the boundary point, all the boundary unknowns should be solved for by either eqn (23) of the U, T method or eqn (24) of the L, M method since no degenerate boundary is present.

To determine the influence coefficient in eqns (23) and (24), we first define the components of the normal vectors as the form

$$n_1(s) = \sin(\theta), \qquad n_2(s) = -\cos(\theta) \tag{33}$$

$$\bar{n}_1(x) = \sin(\phi), \qquad \bar{n}_2(x) = -\cos(\phi) \tag{34}$$

as shown in Fig. 1(a). Then, the inner and cross products are

$$\begin{aligned}\mathbf{n}(x)\cdot\mathbf{n}(s) &= \cos(\phi-\theta)\\ &= \cos(\phi)\cos(\theta)+\sin(\phi)\sin(\theta)\\ &= n_2\bar{n}_2 + n_1\bar{n}_1\end{aligned} \tag{35}$$

$$\begin{aligned}\mathbf{n}(s)\times\mathbf{n}(x)\cdot e_k &= \sin(\phi-\theta)\\ &= \sin(\phi)\cos(\theta)-\cos(\phi)\sin(\theta)\\ &= -\bar{n}_1 n_2 + \bar{n}_2 n_1\end{aligned} \tag{36}$$

Using the following transformation as shown in Fig. 1(b),

$$\begin{Bmatrix} x_r \\ y_r \end{Bmatrix} = \begin{bmatrix} \cos(\theta) & \sin(\theta) \\ -\sin(\theta) & \cos(\theta) \end{bmatrix} \begin{Bmatrix} x_1 - s_1 \\ x_2 - s_2 \end{Bmatrix} \tag{37}$$

The explicit forms of eqns (25)–(28) are shown below:

$$U_{pq} = v\log\sqrt{v^2+y_r^2} - v + y_r\tan^{-1}(v/y_r)\Big|_{v=-0\cdot5L-x_r}^{v=0\cdot5L-x_r} \tag{38}$$

$$\bar{T}_{pq} = \tan^{-1}(v/y_r)\Big|_{v=-0\cdot5L-x_r}^{v=0\cdot5L-x_r} \tag{39}$$

$$\begin{aligned}\bar{L}_{pq} = &-\cos(\phi-\theta)\tan^{-1}(v/y_r)\\ &-0\cdot5\sin(\phi-\theta)\log(v^2+y_r^2)\Big|_{v=-0\cdot5L-x_r}^{v=0\cdot5L-x_r}\end{aligned} \tag{40}$$

$$\begin{aligned}M_{pq} = &\cos(\phi-\theta)\left[\frac{\tan^{-1}(v/y_r)}{y_r}+\frac{v}{v^2+y_r^2}\right]\\ &-y_r\sin(\phi-\theta)\frac{1}{v^2+y_r^2}\\ &-\cos(\phi-\theta)\frac{\tan^{-1}(v/y_r)}{y_r}\Big|_{v=-0\cdot5L-x_r}^{v=0\cdot5L-x_r}\end{aligned} \tag{41}$$

where L is the length of the element. In calculating the above limiting values for a singular element, the L'Hospital rule, inverse triangular relations and the jump function should be considered as follows:

$$\lim_{x\to 0}\frac{x}{\tan^{-1}(x)} = 1 \tag{42}$$

$$\tan^{-1}(x)+\tan^{-1}(1/x) = \pi/2 \tag{43}$$

$$\lim_{y_r \to 0} \tan^{-1}(v/y_r)|_{v=-0\cdot 5L}^{v=0\cdot 5L} = \pi \qquad (44)$$

Therefore, the Cauchy principal value and Hadamard principal value can be easily determined.

For the potential gradient in the x direction on the boundary point, we can determine the potential gradient in the x direction by

$$2\pi \frac{\partial u(x_p)}{\partial x_1} = M_{pq}^{\phi} u_q - \bar{L}_{pq}^{\phi} t_q \qquad (45)$$

where u_q and t_q are all the boundary data, including the boundary conditions and unknown boundary data, which have been solved by eqns (23) or (24), and $\bar{L}_{pq}^{\phi}$ and M_{pq}^{ϕ} are determined by eqns (40) and (41) after substituting $\phi = \pi/2$. In a similar way, the potential gradient in the y direction is determined by

$$2\pi \frac{\partial u(x_p)}{\partial x_2} = M_{pq}^{\phi} u_q - \bar{L}_{pq}^{\phi} t_q \qquad (46)$$

where ϕ in $\bar{L}_{pq}^{\phi}$ and M_{pq}^{ϕ} are set to be π.

AN ILLUSTRATIVE EXAMPLE WITH AN ANALYTICAL SOLUTION AND NUMERICAL IMPLEMENTATION

A benchmark example of test No. 2 in *Boundary Elements Abstracts*,[12] two dimensional steady-state heat conduction with a circular hole in an infinite domain, is considered. The exterior problem satisfies the Laplace equation as follows:

$$\nabla^2 u(r,\theta) = 0, \qquad 1 < r < \infty, \qquad 0 < \theta < 2\pi \qquad (47)$$

with the boundary condition

$$u(r,\theta) = f(\theta), \qquad \text{for } r = 1 \qquad (48)$$

where

$$f(\theta) = \begin{cases} 1\cdot 0, & \text{if } 0 < \theta < \pi \\ -1\cdot 0, & \text{if } \pi < \theta < 2\pi \end{cases} \qquad (49)$$

According to the Poisson integral formula for an exterior domain, the integral representation for the solution can be expressed as

$$u(r,\theta) = \frac{1}{2\pi}\int_0^{2\pi} \frac{r^2 - 1^2}{1^2 + r^2 - 2r\cos(\theta - \theta')} f(\theta')\,d\theta', \quad r > 1 \qquad (50)$$

Substituting the boundary condition of eqn (41) into the Poisson formula and integrating using symbolic math software, the exact solution can be obtained as

$$u(x_1, x_2) = \frac{2}{\pi}\tan^{-1}\left(\frac{2x_2}{x_1^2 + x_2^2 - 1}\right) \qquad (51)$$

and the potential gradients are

$$\frac{\partial u}{\partial x_1} = \frac{2}{\pi}\frac{-4x_1x_2}{(x_1^2 + x_2^2 - 1)^2 + 4x_2^2} \qquad (52)$$

$$\frac{\partial u}{\partial x_2} = \frac{2}{\pi}\frac{2(x_1^2 + x_2^2 - 1) - 4x_2^2}{(x_1^2 + x_2^2 - 1)^2 + 4x_2^2} \qquad (53)$$

To check the exact solution of eqn (50), a bilinear transformation in conformal mapping is also employed to confirm the exact solution. The two processes of conformal mapping are shown below:

$$w_1 = \frac{z-1}{z+1} \qquad (54)$$

$$w_2 = \ln(w_1) \qquad (55)$$

where z, w_1 and w_2 are complex functions.

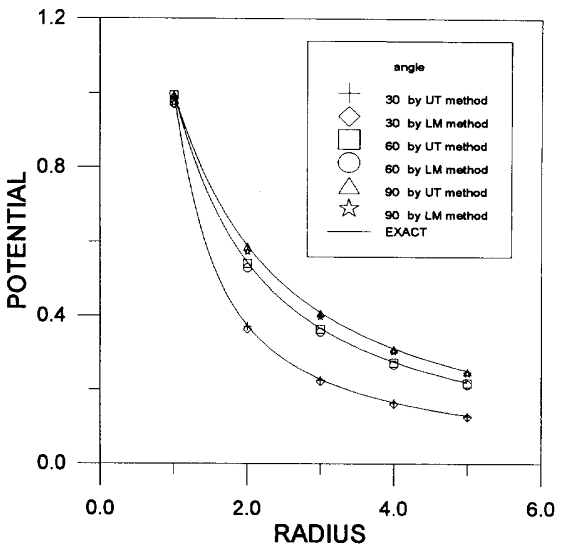

Fig. 3. Potential distribution along 30, 60 and 90° by using the U, T and L, M methods.

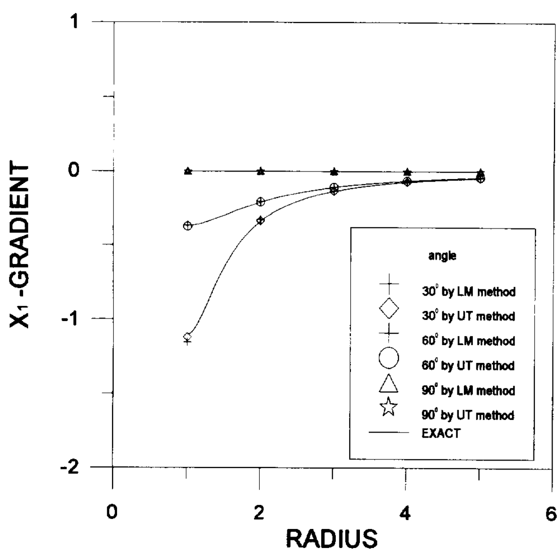

Fig. 4. Potential gradient in the x_1 direction along 30, 60 and 90° by using the U, T and L, M methods.

Substituting z by $x_1 + x_2 i$ into w_1 in eqn (54), we have

$$w_1 = \frac{x_1^2 + x_2^2 - 1 + 2x_2 i}{(x_1 + 1)^2 + x_2^2} \tag{56}$$

Since w_1 is on the unit circle, eqn (55) can be reduced to

$$w_2 = i \arg(w_1) \tag{57}$$

where arg denotes the argument of a complex number. Therefore, the solution of $u(x_1, x_2)$ in eqn (51) can be derived again.

In eqns (52) and (53), it is easily found that the potential gradient at the boundary points $(1,0)$ and $(-1,0)$ does not exist since the potential discontinuity is present near these two points. Also, a series solution has been presented in Ref. 12 as follows:

$$u(r,\theta) = a_0 + \sum_{n=1}^{\infty} (a_n \cos(n\theta) + b_n \sin(n\theta)) r^{-n}$$

where

$$a_0 = a_n = 0$$

$$b_n = \frac{2}{n\pi}[1 - (-1)^n]$$

Since more than 40 terms were needed to reach the convergence found in Ref. 12, the solution is not adopted in the following numerical calculations.

In numerical implementation, two alternatives are suggested to modify the program, BEPO2D, for an interior problem from interior problems to exterior problems: change the connectivity of the boundary element as shown in Fig. 2, or modify the program using eqns (31) and (32). Both alternatives result in the same influence coefficients. Therefore, only one numerical result will be shown.

RESULTS AND DISCUSSION

Based on the three versions for the exterior problem, the linear algebraic equations are found to be the same. The numerical example is test problem no. 2 in ISBE benchmarks for steady state heat conduction for the exterior problem. The 24 boundary elements are shown in Fig. 2. The potential distributions along 30, 60 and 90° are shown in Fig. 3, and the boundary element solution agrees with the exact solution very well. Also, in Figs 4 and 5, the numerical results of the potential gradient in the x_1 and x_2 directions along 30, 60 and 90° for the interior point are satisfactory. Furthermore, the potential gradients in the x and y directions on the boundary point are determined by eqns (45) and (46) and are shown in Figs 6 and 7, respectively. All the above DBEM results were obtained by using the U, T or L, M methods. Both methods agree with the exact solution. It is found that oscillation occurs near the zero angle in Figs 6 and 7 due to the singular point at $(1,0)$. The potential flux approaches infinity at these two points, $(1,0)$ and $(-1,0)$ in the (x,y) coordinate system as eqns (45) and (46) reveal, since potential discontinuity is present at the two points. However, calculation of the potential gradient at the other points along the circular boundary is carried out instead of failure in Ref. 12. The normal fluxes on the $r = 1$ boundary, and the $r = 2$ and $r = 3$ artificial boundaries

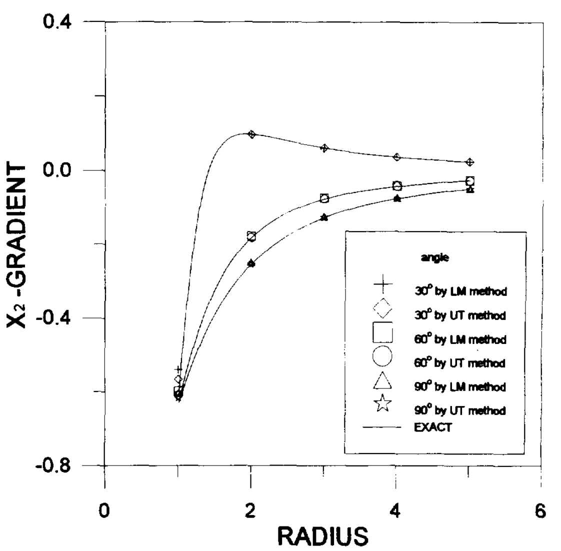

Fig. 5. Potential gradient in the x_2 direction along 30, 60 and 90° by using the U, T and L, M methods.

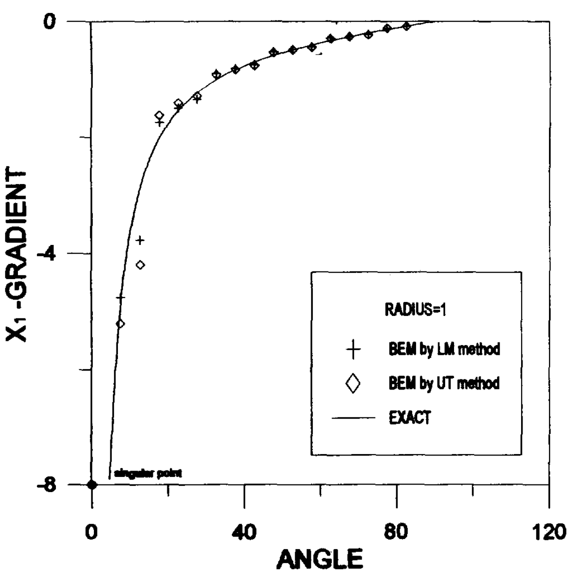

Fig. 6. Potential gradient in the x_1 direction on the circular boundary by using the U, T and L, M methods.

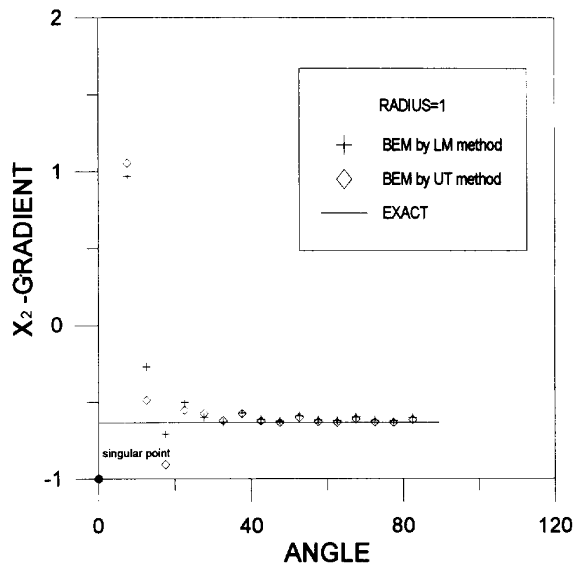

Fig. 7. Potential gradient in the x_2 direction on the circular boundary by using the U, T and L, M methods.

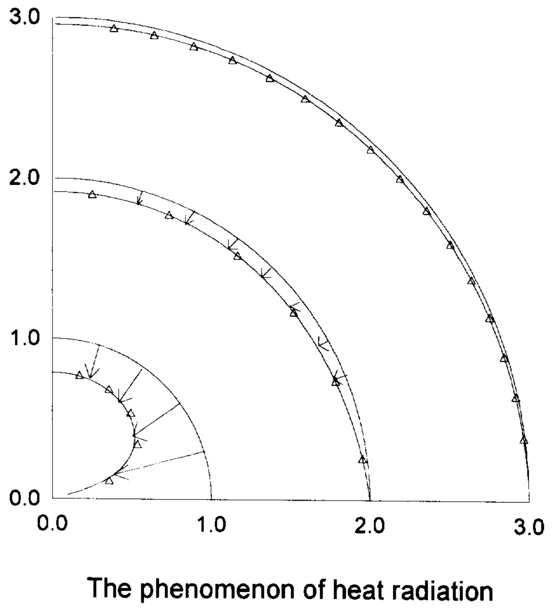

Fig. 8. Normal flux along the $r = 1, 2$ and 3 boundaries.

are shown in Fig. 8. It is found that the larger distance r is, the smaller is the normal flux obtained. This result obeys the law of heat balance.

CONCLUSIONS

Three versions of dual integral formulations for the exterior problems have been proposed. It has been found that the free term for the third version is different from that of the interior problem. The relations of the linear algebraic equations for the interior and exterior problems have been discussed. Two alternatives have been incorporated into the program, BEPO2D, for the interior problem to solve the exterior problem. A benchmark example of test No. 2 in *Boundary Elements Abstracts* has been used to show the validity of the present formulations. Also, the failure to determine the potential gradient on the boundary point has been dealt with by the proposed dual formulations.

REFERENCES

1. Chen, J. T. On Hadamard principal value and boundary integral formulation of fracture mechanics. Master's thesis, Institute of Applied Mechanics, National Taiwan University, 1986.
2. Hong, H.-K. & Chen, J. T. Derivation of integral equations in elasticity. *J. Engng Mech. Div., ASCE*, 1988, **114**(6), Em5, 1028–44.
3. Chen, J. T. & Hong, H.-K. On the dual integral representation of boundary value problem in Laplace equation. *Boundary Elements Abstracts*, 1993, **4**(3), 114–16.
4. Chen, J. T., Hong, H.-K. & Chyuan, S. W. Boundary element analysis and design in seepage flow problems with sheetpiles. *Finite Elements in Analysis and Design*, 1994, **17**, 1–20.
5. Portela, A., Aliabadi, M. H. & Rooke, D. P. The dual boundary element method: effective implementation for crack problems. *Int. J. Num. Meth. Engng*, 1992, **33**, 1269–87.
6. Mi, Y. & Aliabadi, M. H. Dual boundary element method for three dimensional fracture mechanics analysis. *Engineering Analysis with Boundary Elements*, 1992, **10**(2), 161–71.
7. Fedelinski, P. & Aliabadi, M. H. The dual boundary element method: *J*-integral for dynamic stress intensity factors. *Int. J. Fracture*, 1994, **65**(4), 369–81.
8. Leitao, V., Aliabadi, M. H. & Rooke, D. P. The dual boundary element formulation for elastoplastic fracture mechanics. *Int. J. Num. Meth. Engng*, 1995, **38**, 315–33.
9. Chen, W. H. & Chen, T. C. An efficient dual boundary element technique for a two-dimensional fracture problem with multiple cracks. *Int. J. Num. Meth. Engng*, 1995, **38**, 1739–56.
10. Chen, J. T. & Hong, H.-K. Dual boundary integral equations at a corner using contour approach around singularity. *Advances in Engineering Software*, 1994, **21**(3), 169–78.
11. Chen, J. T. & Hong, H.-K. *Boundary Element Method*, 2nd edn. New World Press, Taipei, Taiwan, 1992 (in Chinese).
12. Test no. 2, Two dimensional steady state heat conduction with a circular boundary in an infinite domain. *Boundary Elements Abstracts*, 1990, **1**(2), 90–1.
13. Brebbia, C. A., Telles, J. C. F. & Wrobel, L. C. *Boundary Element Techniques — Theory and Applications in Engineering*. Springer-Verlag, Berlin, 1984.